Influence of Crystallinity on the Dielectric Relaxation Behavior of Poly(ether ether ketone)

Douglass S. Kalika* and Rajendra K. Krishnaswamy

Department of Chemical Engineering, University of Kentucky, Lexington, Kentucky 40506-0046

Received September 15, 1992; Revised Manuscript Received May 13, 1993

ABSTRACT: The dielectric relaxation characteristics of amorphous and semicrystalline poly(ether ether ketone) have been investigated as a function of crystallization history; both the glass–rubber (α) relaxation and a sub-glass (β) relaxation were examined. The characteristics of the α relaxation were highly sensitive to crystallinity owing to the constraint imposed on the amorphous phase dipoles by the presence of the crystalline phase. The magnitude of the α relaxation strength indicated an immobilized rigid amorphous phase fraction in the semicrystalline samples which appeared to relax at temperatures above T_g; finite rigid amorphous fractions were observed for both cold-crystallized and melt-crystallized specimens. The sub-glass (β) relaxation was also sensitive to the presence of crystallinity: the isochronal loss maxima measured for the cold-crystallized samples were offset to higher temperatures as compared to the wholly-amorphous material, and a disproportionate decrease in the β relaxation strength with the degree of crystallinity was observed. The influence of the crystalline phase on the β relaxation thus appears to extend well into the amorphous material, suggesting sub-glass motions which encompass a larger segmental length scale as compared to more flexible polymers.

Introduction and Background

The advent of a range of engineering thermoplastics based on primarily aromatic backbone structures and encompassing outstanding mechanical and thermal properties has created an opportunity for the application of melt-processable materials in a variety of areas where such resins have not traditionally been employed. In the area of structural composites, for example, such engineering thermoplastics have been seen as potential replacements for thermosetting matrices, the thermoplastics offering a relative ease of processing and enhanced toughness while overcoming deficiencies in end-use temperature and solvent resistance typically attributed to thermoplastics. A primary candidate for structural composite applications in this regard is poly(ether ether ketone) (PEEK). The successful application of PEEK for composites requires a detailed knowlege of how processing conditions and material history influence the resultant semicrystalline morphology and how this morphology ultimately impacts bulk composite properties (mechanical strength, chemical and thermal resistance, long-term stability, etc.).

The development of crystalline structure and morphology in PEEK has been investigated extensively over the past decade and is the subject of a recent review.[1] A number of detailed thermal analysis studies have appeared which serve to elucidate the complex crystallization behavior of the neat material.[2-12] These studies, based primarily on differential scanning calorimetry (DSC), indicate material thermal characteristics which are a strong function of crystallization history. One of the more striking features reported for crystalline PEEK samples is the observed "double melting" behavior, wherein DSC heating sweeps of isothermally cold-crystallized or melt-crystallized samples display two distinct melting endotherms: a "low-temperature" endotherm located approximately 15–20 °C above the imposed isothermal crystallization temperature and a high-temperature endotherm, with a peak position essentially independent of annealing temperature. This behavior has been attributed to established morphological features[3,13] and possible crystal reorganization during the scan itself.[4] Melt-crystallization studies by Cheng and co-workers[2] clearly indicate that the high-melting crystals evolve first, followed by the low-melting fraction, thus establishing the behavior independent of structural reorganizations encountered during subsequent heating. Combined microscopy and calorimetric investigations by Bassett et al.[3] reveal two distinct lamellar populations corresponding to the two melting peaks: the high-temperature endotherm corresponds to melting of the dominant, primary lamellae within the spherulitic texture, while the low-temperature endotherm corresponds to melting of secondary lamellae located between the primary lamellae. Recent optical studies by Marand and Prasad[13] on PEEK films of relatively low nucleation density also reveal the evolution of two distinct morphological populations: at low melt crystallization temperatures and short times a spherulitic texture is observed, while at longer times and somewhat higher crystallization temperatures an additional "crystal-aggregate-like" morphology is seen to develop. These secondary structures nucleate predominantly at the edge of the initial spherulites, their growth proceeding along the spherulite radius. The increase in the relative volume of the secondary structures as a function of crystallization time has led to their correlation with the characteristic double-melting behavior, the crystal-aggregate population corresponding to the low-temperature endotherm, and the initial spherulitic population corresponding to the high-temperature endotherm.

Crystallization kinetics determined by bulk calorimetric measurements appear to be consistent with the morphological observations described above. For short isothermal crystallization times, both cold-crystallization and melt-crystallization processes follow an Avrami dependence,[5-9] with logarithmic plots of $-\ln(1 - X_c(t)/X_c(\infty))$ versus time providing a linear result with slope n (the Avrami exponent); $X_c(t)$ and $X_c(\infty)$ represent the bulk crystallinity at time t and at the end of crystallization, respectively. Investigation of commercial PEEK samples reveals values of n close to 3,[5,6] which is consistent with simultaneous nucleation and a spherulitic growth process. Kinetic studies on a series of PEEK samples with a range of molecular weights indicate a melt-crystallization Avrami exponent $n = 2$,[7] which may reflect the development of a disklike morphology. At longer crystallization times, a second linear region is observed with a lower slope

0024-9297/93/2226-4252$04.00/0

corresponding to the predominance of a secondary crystallization process. Velisaris and Seferis[8] and later Cebe[9] analyzed the overall two-slope behavior in both neat PEEK and carbon fiber reinforced PEEK using a dual crystallization Avrami expression encompassing two separate crystallization processes occurring in parallel; process 1, which dominates at short times, had a corresponding Avrami exponent $n \sim 2.5$, while process 2, which dominates at longer times, had an Avrami exponent $n \sim 1.5$. Cebe[9] assigned process 1 (fast) to the high-temperature DSC endotherm and process 2 (slow) to the low-temperature DSC endotherm, consistent with the results of Cheng.[2]

The glass transition behavior of PEEK is also highly sensitive to the crystalline morphology of the material as governed by thermal history. Upon heating across the glass transition, the increase in amorphous phase chain mobility as reflected by the measured increase in heat capacity (ΔC_p) is considerably less than that expected based on full mobilization of the noncrystalline material.[2,14] This has led to the assignment of a "rigid amorphous phase" (RAP) fraction in PEEK, which corresponds to the difference between the overall rigid fraction representing all material which remains solidlike (i.e., immobile) across T_g and the fully crystalline fraction determined by melting enthalpy measurements. Rigid amorphous portions have been observed in thermal analysis studies of polypropylene[15] and poly(oxymethylene)[16,17] and for polymers with less flexible structures such as poly(phenylene sulfide) (PPS).[18-20] The relative fraction of rigid amorphous material which is measured in semicrystalline PEEK reflects the conditions of crystallization, with more restrictive crystallization conditions (i.e., lower isothermal crystallization temperatures or faster cooling rates for nonisothermal crystallization), leading to a higher rigid amorphous phase fraction. Isothermal cold crystallizations by Cheng et al.[2] in the range 190–270 °C reveal rigid amorphous phase fractions at the glass transition which decrease continuously with increasing annealing temperature, from 0.14 to 0.08; these values represent approximately 32% and 17% of the total rigid fraction, respectively. The calorimetric glass transition temperature decreases with decreasing rigid amorphous fraction. Cold-crystallization studies by Huo and Cebe[14] indicate a similar result, although with higher levels of the rigid amorphous phase fraction observed across a comparable range of annealing temperatures (χ_{RAP} decreasing from 0.32 to 0.24 with increasing annealing temperature). Melt-crystallization studies by Cheng and co-workers[2] were carried out for both isothermal and nonisothermal crystallization histories. Samples cooled from the melt at varying rates revealed rigid amorphous phase fractions which were somewhat lower than those encountered during cold crystallization and which decreased with decreasing cooling rate. For samples which were isothermally crystallized in the melt over long times (290–320 °C), no rigid amorphous phase fraction was evident from subsequent calorimetric measurements.

In addition to the quantitative determination of the rigid amorphous phase fraction at the glass transition, the possible mobilization of the rigid amorphous material at temperatures between T_g and the melting temperature (T_m) has been investigated.[2,14-19] In the case of PEEK and PPS, initial calorimetric investigations indicated no relaxation of the rigid amorphous material prior to melting;[2,18] these observations were complicated by the low-temperature melting behavior of samples containing a sizable rigid amorphous fraction. Dielectric studies by Huo and Cebe,[14,19] however, clearly demonstrated a progressive mobilization of rigid amorphous material above the glass transition for both PEEK and PPS. Specifically, the measured dielectric relaxation strength was observed to increase with temperature above the glass transition for a series of cold-crystallized specimens of varying crystallinity, consistent with the gradual relaxation of the rigid amorphous phase (see below).

The dynamic relaxation behavior of poly(ether ether ketone) has been investigated by both dielectric[14,21-23] and dynamic mechanical methods.[23-26] PEEK displays a broad, sub-glass relaxation at low temperatures (designated here as the β relaxation) in addition to its glass–rubber (α) relaxation. The most extensive dielectric study of the α relaxation in PEEK was reported by Huo and Cebe,[14] who investigated the relaxation behavior for both the amorphous material and a series of cold-crystallized specimens. Their results were largely consistent with the behavior reported for low-crystallinity polymers in general (e.g., for PET, see Boyd[27,28]): the presence of the crystalline phase resulted in a significant broadening of the α relaxation as compared to the initially-amorphous sample, as well as a positive offset in the isochronal relaxation temperature. These phenomena reflect the marked influence of the crystallites on the long-range segmental mobility of the amorphous chains in the rubbery state. Dielectric relaxation strength was observed to decrease with increasing crystallinity, and, as noted above, a progressive relaxation of some portion of the rigid amorphous material was observed in the semicrystalline samples above T_g, as evidenced by an increase in the dielectric relaxation intensity with temperature over this range.

Dielectric studies of the β relaxation in PEEK have been limited to wholly-amorphous samples. Specifically, Starkweather and Avakian[21] reported Arrhenius plots for the β relaxation in amorphous PEEK as measured by both dielectric and dynamic mechanical methods. They observed that the maximum in tan δ occurred at higher frequencies (lower temperatures) in the dielectric studies as compared to the dynamic mechanical experiments and that the corresponding apparent activation energy for the dielectric data was nearly a factor of 2 lower as compared to the dynamic mechanical results. It was concluded that the dielectric relaxation represents a high-frequency, low-temperature component of a broader distribution of motions as observed in the dynamic mechanical studies. Further, the relative values of the activation energy suggest that the dielectric relaxation reflects highly-localized, noncooperative motions of small chain fragments, while the dynamic mechanical relaxation encompasses a wider range of segmental motion of a more cooperative nature. Low-temperature dynamic mechanical data reported by Sasuga and Hagiwara[25,26] are consistent with these observations; studies of both amorphous PEEK and a single semicrystalline sample reveal a very broad sub-glass relaxation which the authors attribute to a combination of up to three different, overlapping molecular processes. To date, no systematic exploration of the influence of varying crystallinity on the dynamic mechanical properties of PEEK has appeared.

In this work, the dielectric characteristics of amorphous and both cold-crystallized and melt-crystallized PEEK specimens have been investigated over a wide range of frequency and temperature; both the glass–rubber (α) and sub-glass (β) relaxations have been examined. As anticipated, the dielectric response characteristics of the α transition were highly sensitive to crystallization history, with relaxation strength and temperature reflecting the

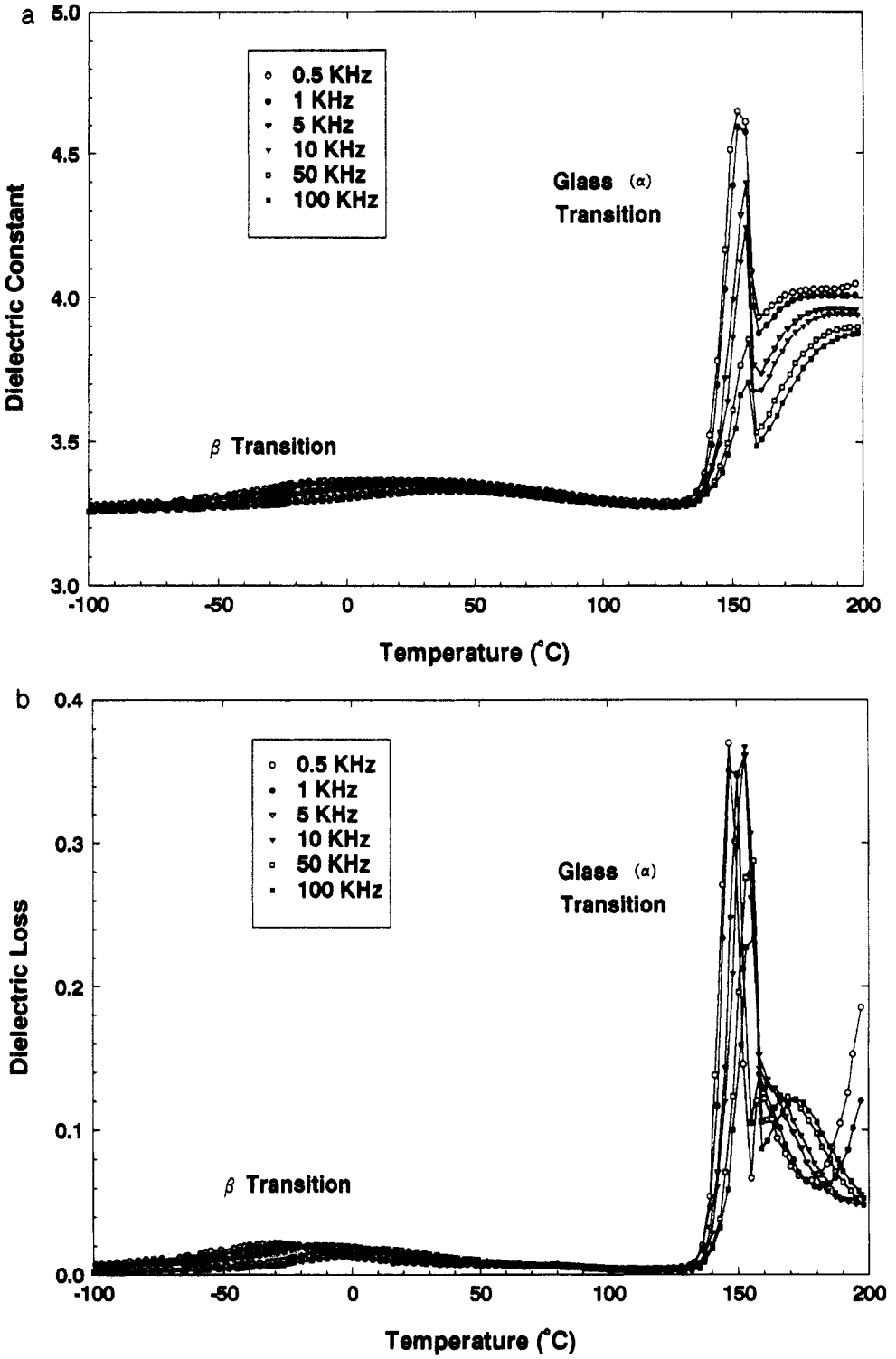

Figure 1. Dielectric results for amorphous PEEK: (a) dielectric constant (ϵ') versus temperature (°C); (b) dielectric loss (ϵ'') versus temperature (°C). (○) 0.5, (●) 1, (▽) 5, (▼) 10, (□) 50, (■) 100 kHz.

complex morphological features of the material. The dielectric characteristics of the β relaxation were also sensitive to the presence of crystallinity, in contrast to behavior observed for more flexible polymers.[27] The isochronal loss peak temperatures measured for the semicrystalline samples were offset significantly relative to those measured for the amorphous material, and the β relaxation strength in the semicrystalline specimens was diminished disproportionately relative to the weight fraction of crystallinity present. These results indicate that the crystalline phase has a far-reaching impact on the molecular motions inherent to the β relaxation and that the spatial extent of these motions is greater than would be expected for sub-glass relaxations in general.

Experimental Methods

PEEK samples were obtained as both amorphous film (Stabar K200, 0.10-mm thickness) and pellets ("Victrex" 450G) from ICI Films and ICI Advanced Materials, respectively. Cold-crystallized samples of varying crystallinity were achieved by annealing the K200 film in a temperature-controlled Carver melt press at temperatures ranging from 175 to 300 °C. All samples were isothermally annealed for 45 min. Melt-crystallized specimens (thickness of approximately 0.13 mm) were obtained by compression molding the 450G pellets from the melt at moderate pressure (melt temperatures ranging from 350 to 400 °C), with subsequent cooling to the solid state at a constant rate (~1 °C/min) or in a stepwise manner (1-h isothermal intervals). The resulting crystalline fraction was determined based on density gradient measurements (carbon tetrachloride/toluene column);

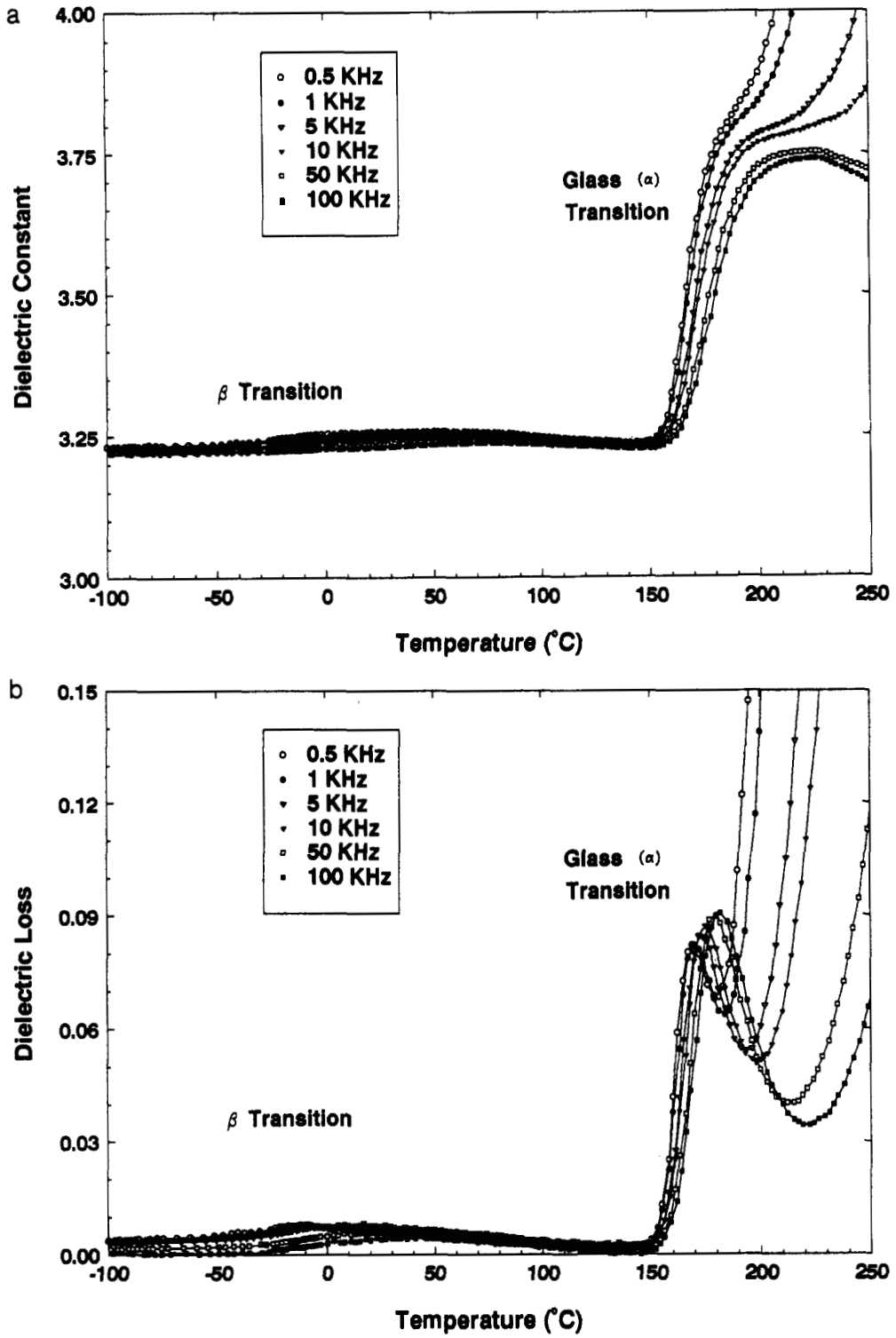

Figure 2. Dielectric results for cold-crystallized PEEK (T_a = 225 °C; W_c = 0.29). (a) dielectric constant (ϵ') versus temperature (°C); (b) dielectric loss (ϵ'') versus temperature (°C). (○) 0.5, (●) 1, (▽) 5, (▼) 10, (□) 50, (■) 100 kHz.

the density of the amorphous (as-received) film was determined to be ρ_a = 1.258 g/cm^3, and the crystal density was taken as ρ_c = 1.400 g/cm^3.[29]

Dielectric spectroscopy measurements were accomplished using a Polymer Laboratories dielectric thermal analyzer (PL-DETA) composed of a GenRad Digibridge interfaced with the Polymer Laboratories temperature controller. Silver electrodes (33 mm) were vacuum evaporated directly on the samples, which were held between polished platens in the temperature-controlled test oven. All samples were dried under vacuum prior to measurement and were investigated in an inert atmosphere. The dielectric constant (ϵ') and loss factor (tan δ) were recorded at frequencies ranging from 50 Hz to 100 kHz across a temperature range of −100 to +300 °C; the dielectric scanning rate was 1.5 °C/min. Supplementary thermal analysis was accomplished using differential scanning calorimetry (Perkin-Elmer DSC-7, scanning rate of 20 °C/min).

Results

The dielectric results for the amorphous PEEK sample are plotted isochronally as dielectric constant and loss versus temperature in Figure 1. The material displays a broad sub-glass (β) relaxation at low temperatures and a dramatic increase in the dielectric constant in the vicinity of the glass transition (α relaxation). The dielectric constant decreases sharply at approximately 160 °C corresponding to the onset of crystallization, with a recovery in ϵ' observed at higher temperatures. Examination of the dielectric loss in the vicinity of the glass

transition reveals a narrow relaxation peak corresponding to the mobilization of the initially-amorphous material with increasing temperature. Subsequent nonisothermal cold-crystallization (above 160 °C) produces a positive offset in the relaxation temperature of the now-constrained mobile amorphous fraction, and the eventual relaxation of this portion of the material with increasing temperature is evident as a broad but distinct shoulder in dielectric loss located on the high-temperature side of the glass transition loss peak.

Dielectric results for a representative cold-crystallized sample (T_a = 225 °C) are shown in Figure 2. The shape of the β relaxation is largely unchanged as compared to the amorphous result, with a decrease in magnitude evident corresponding to the constraining influence of the crystalline fraction. Also, a positive offset in the isochronal peak temperatures is observed, T_β (1 kHz) increasing by approximately 18 °C, independent of crystallinity (see details below). The α relaxation is indicated by a stepwise increase in the dielectric constant at the higher frequencies investigated; a corresponding broad dielectric loss peak is evident in Figure 2b and is offset to higher temperatures as compared to the amorphous specimen. The dramatic increase in dielectric constant and loss observed above the glass transition at the lower frequencies is due to the onset of ionic conductivity in the multiphase sample. The influence of ionic conductivity was removed from the dielectric loss data prior to analysis using methods described previously.[30]

Dielectric measurements from all samples were analyzed for both the α and β relaxations through the construction of Argand plots of dielectric loss versus dielectric constant; results for the amorphous sample are shown by way of example in Figure 3. Data for both the amorphous and semicrystalline specimens can be described by the symmetric Cole–Cole modification of the Debye equation, whereby the complex dielectric constant, ϵ^*, is related to the relaxed (ϵ_r) and unrelaxed (ϵ_u) values of the dielectric constant, the frequency (ω), a central relaxation time (τ), and a symmetric broadening parameter (β'):[31]

$$\epsilon^* = \epsilon_u + \frac{\epsilon_r - \epsilon_u}{1 + [i\omega\tau]^{\beta'}} \quad (1)$$

The semicircular arcs in Figure 3 represent least-squares fits to eq 1.

A summary of the crystallinity and relaxation characteristics of the various cold-crystallized samples is provided as a function of the isothermal annealing temperature in Table I. The level of crystallinity (W_c) is reported on a weight fraction basis as determined by density gradient measurements. Attempts to quantify bulk crystallinity in these samples using calorimetric methods were unsuccessful, owing to complications introduced by the occurrence of additional cold crystallization during the calorimetric sweeps.[12] A calorimetric glass transition temperature (T_g, 20 °C/min) is reported in conjunction with the α relaxation results in Table I.

Examination of the results for the cold-crystallized samples indicates a systematic increase in the weight fraction crystallinity with annealing temperature, with a maximum level of 37% crystallinity achieved for T_a = 300 °C. As noted, the isochronal peak temperatures corresponding to the α relaxation (reported here at a frequency of 1 kHz) are significantly higher for the crystallized samples as compared to the initially-amorphous material; the peak temperature (T_α) displays a relative maximum for the T_a = 200 °C specimen and decreases for samples of higher crystallinity. This behavior is mirrored by the

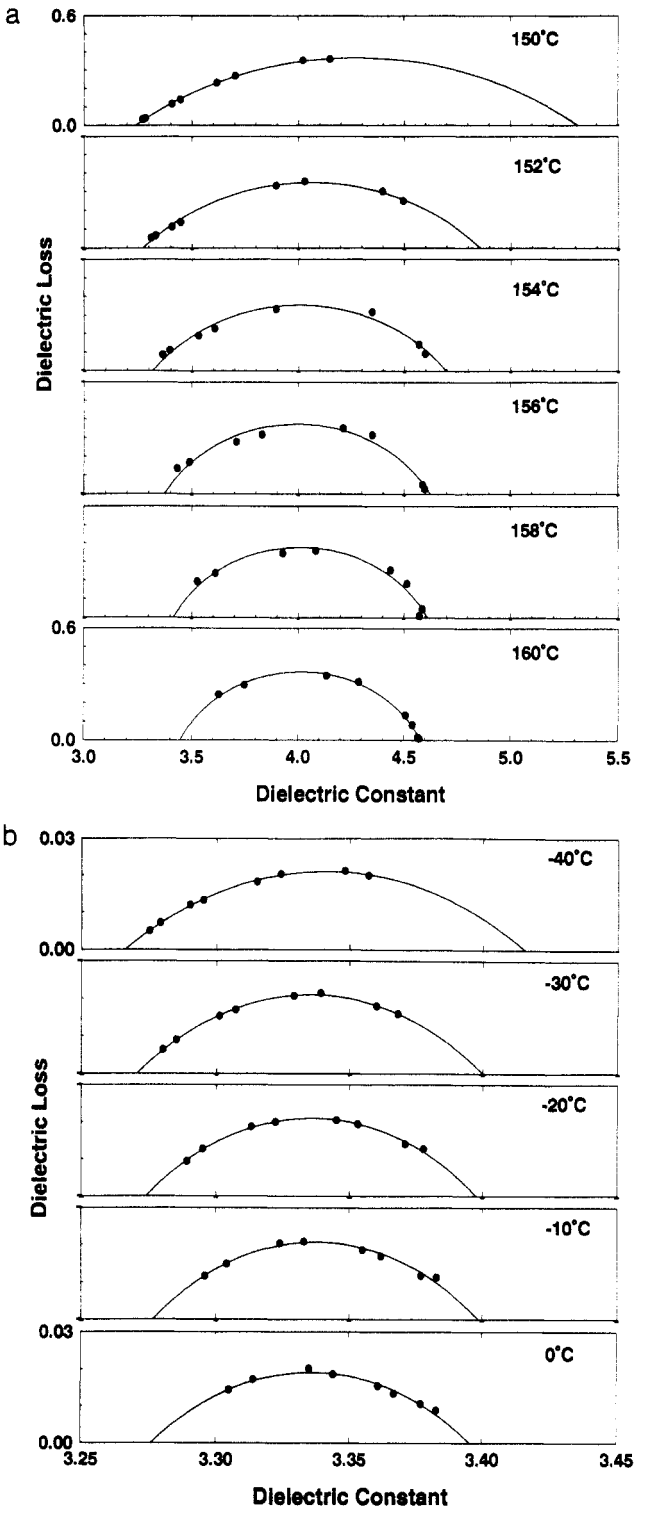

Figure 3. Argand plots for amorphous PEEK: (a) α relaxation range; (b) β relaxation range. Semicircular arcs represent least-squares fits to the Cole–Cole equation.

calorimetric data (T_g) and is in qualitative agreement with both the calorimetric and dielectric results reported by Cheng et al.[2] and Huo and Cebe,[14] respectively. The overall dielectric relaxation strength ($\Delta\epsilon$, evaluated at T_α) decreases with increasing crystalline fraction.

Results for the sub-glass (β) relaxation indicate an amorphous specimen relaxation strength ($\Delta\epsilon(T_\beta)$) for this transition which is an order of magnitude lower than that observed at the glass–rubber relaxation. The presence of a finite crystalline fraction causes a positive offset in the measured isochronal relaxation temperature and a corresponding decrease in relaxation strength. Both T_β and $\Delta\epsilon$ appear to be relatively insensitive to the bulk crystalline

Table I. Dielectric Characteristics of the β and α Relaxations[a]

	T_a (°C)	W_c	T_β (°C)	$\Delta\epsilon(T_\beta)$	T_α (°C)	$\Delta\epsilon(T_\alpha)$	T_g (°C)
A		0.0	−28	0.130	155.0	1.37	146.6
1	175	0.24	−10	0.046	165.0	0.69	159.2
2	200	0.26	−10	0.044	168.5	0.66	158.7
3	225	0.29	−10	0.047	167.5	0.58	158.4
4	250	0.31	−10	0.044	166.0	0.58	157.4
5	275	0.34	−12	0.047	165.0	0.53	157.2
6	300	0.37	−7	0.032	163.5	0.52	154.3

[a] T_a (°C), isothermal cold-crystallization annealing temperature; W_c, weight fraction crystallinity based on density gradient measurements; T_β (°C), isochronal peak temperature measured at 1 kHz (β relaxation); $\Delta\epsilon(T_\beta) = \epsilon_r - \epsilon_u$, dielectric relaxation strength evaluated at T_β; T_α (°C), isochronal peak temperature measured at 1 kHz (α relaxation); $\Delta\epsilon(T_\alpha) = \epsilon_r - \epsilon_u$, dielectric relaxation strength evaluated at T_α; T_g (°C), glass transition temperature measured by calorimetry (20 °C/min, DSC).

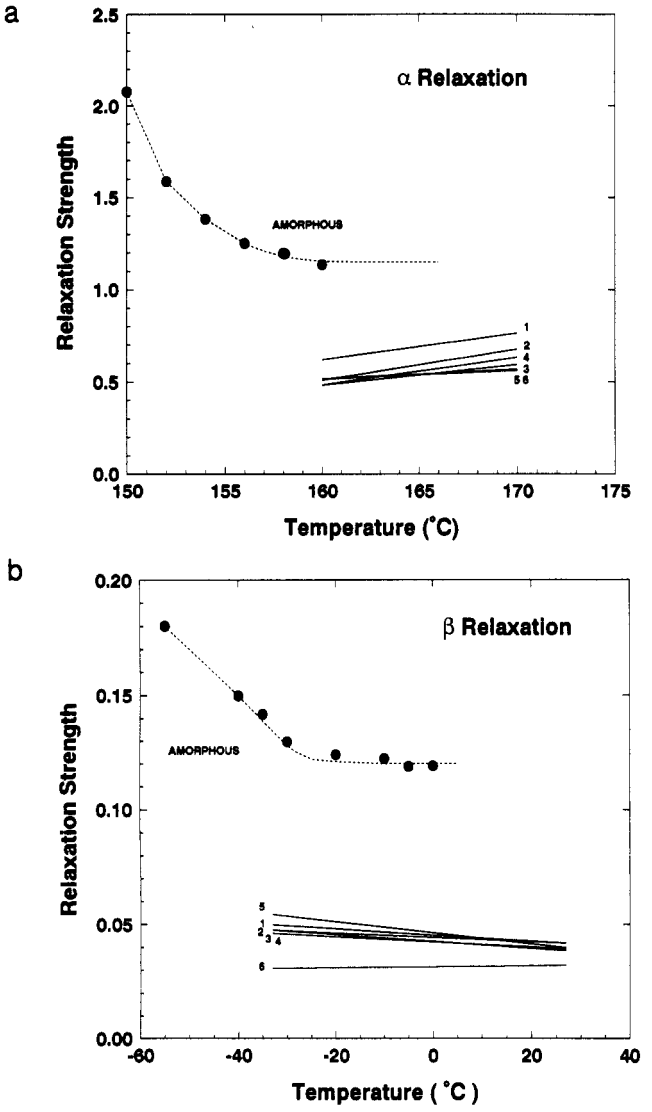

Figure 4. Dielectric relaxation strength ($\Delta\epsilon = \epsilon_r - \epsilon_u$) versus temperature (°C): (a) α relaxation; (b) β relaxation. Amorphous and cold-crystallized samples, with sample labels according to Table I.

level in the cold-crystallized samples; T_β (1 kHz) remains approximately constant at −10 °C across the range of cold crystallinities, with $\Delta\epsilon \sim 0.045$. $\Delta\epsilon$ does decrease significantly for the T_a = 300 °C sample, however.

The temperature dependence of the Cole–Cole parameters ($\Delta\epsilon$, β') for the two relaxations is reported in Figures 4 and 5. The relaxation strength of the amorphous sample in the vicinity of the glass (α) transition is strongly

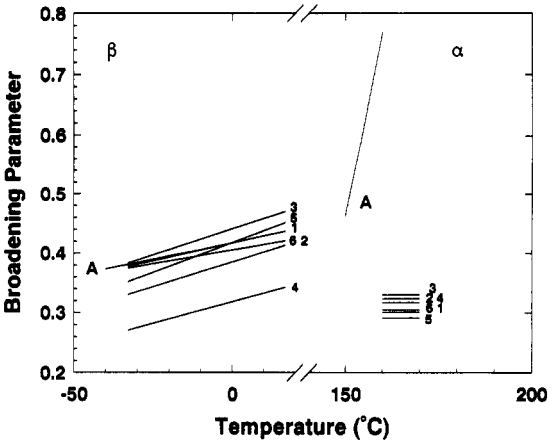

Figure 5. Cole–Cole broadening parameter (β') versus temperature (°C) for α and β relaxations. Amorphous and cold-crystallized samples, with sample labels according to Table I.

temperature-dependent, $\Delta\epsilon$ decreasing with increasing temperature and approaching a plateau value just prior to the onset of cold crystallization (Figure 4a). Across this same temperature range the relaxation narrows significantly, as evidenced by a sharp increase in the broadening parameter (β'). Results for the cold-crystallized samples in the vicinity of the α relaxation do not display nearly as strong a temperature dependence. The dielectric relaxation strength increases with temperature for all cold-crystallized samples, with the vertical offset in the sample curves reflecting the overall decrease in $\Delta\epsilon$ as a function of the crystalline fraction; these results are in agreement with the observations of Huo and Cebe,[14] the increase in dielectric relaxation strength with increasing temperature corresponding to the gradual mobilization of dipoles in the rigid amorphous phase. The magnitude of the temperature dependence, as reflected in the slope of the $\Delta\epsilon$ versus temperature curves, appears to decrease with increasing sample crystallinity. The Cole–Cole broadening parameter is essentially temperature-independent for the cold-crystallized samples (α relaxation) and is considerably reduced as compared to the amorphous specimen.

Consideration of the dielectric relaxation strength as a function of temperature and bulk crystallinity for the β relaxation (Figure 4b) indicates a decrease in $\Delta\epsilon$ with increasing temperature for both the amorphous and cold-crystallized samples; the amorphous sample behavior is similar to the α relaxation result, with relaxation strength decreasing and then approaching a nearly constant value with increasing temperature. In the crystallized specimens, $\Delta\epsilon$ decreases continuously in the region of the subglass relaxation, reflecting a decrease in the orientational polarizability of the responding dipoles with increasing temperature. The Cole–Cole broadening parameter is seen to increase with temperature for all samples investigated, corresponding to a progressive narrowing of the β relaxation (Figure 5).

Arrhenius plots of log{frequency} versus $1/T_{max}$ based on the isochronal loss data are shown in Figure 6. α relaxation data corresponding to the amorphous sample and selected cold-crystallized samples are plotted in Figure 6a; the positive offset in transition temperature for the crystallized samples is reflected in a shift of the data to the left. High-frequency data for the amorphous sample (≥50 kHz) display a shift to lower peak temperatures (higher $1/T_{max}$) as compared to the trend of the low-frequency results owing to the influence of cold crystallization on the nonisothermal dielectric sweeps. Both the amorphous and crystalline results can be satisfactorily

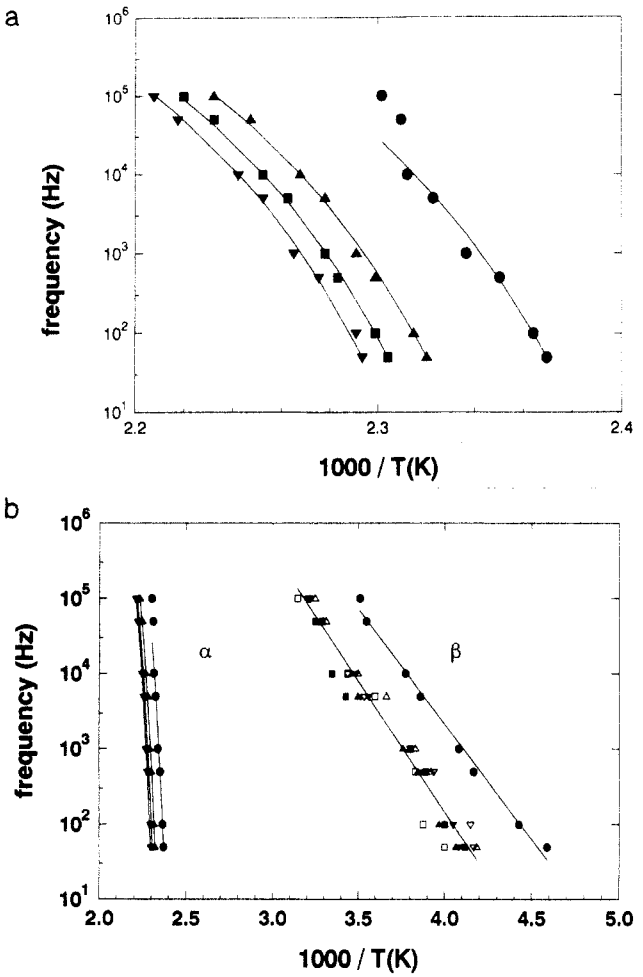

Figure 6. Arrhenius plots of frequency (Hz) versus $1000/T$ (K) based on isochronal temperature sweeps; amorphous and cold-crystallized PEEK: (a) α relaxation; (b) combined α and β relaxations. (●) Amorphous PEEK, (▽) T_a = 175 °C, (▼) T_a = 200 °C, (□) T_a = 225 °C, (■) T_a = 250 °C, (△) T_a = 275 °C, (▲) T_a = 300 °C. Solid curves represent WLF fit (α relaxation).

described using a single WLF-type expression (see plot). The activation energy for the amorphous sample ranges from 1065 kJ/mol (50 Hz) to 455 kJ/mol (100 kHz), as reflected in the local slope of the data across the frequency range of investigation. The activation energies observed for the various cold-crystallized samples are largely independent of the bulk level of crystallinity and range from 1125 kJ/mol (50 Hz) to 480 kJ/mol (100 kHz). These values are comparable in magnitude to the (frequency-independent) estimates reported by Cebe.[14]

Combined results for both the α and β relaxations are shown in Figure 6b. The β relaxation data display a linear Arrhenius behavior which is characteristic of sub-glass relaxations;[31] data for the cold-crystallized samples show the observed offset to higher temperatures, with all of the (cold-crystallized) results falling in a single band. An apparent activation energy of 58 kJ/mol is indicated for the amorphous sample, which is somewhat higher than the dielectric-based value reported by Starkweather and Avakian[21] (42–46 kJ/mol) over the same range of frequencies. The cold-crystallized samples display an aggregate activation energy of 66 kJ/mol.

In addition to the cold-crystallized specimens detailed above, PEEK samples with various melt-crystallization histories were examined. Specifically, samples were prepared by compression molding of PEEK pellets at melt temperatures of 350, 375, and 400 °C (time at $T_m \sim 10$ min), with subsequent melt crystallization; calorimetric

Table II. Dielectric Characteristics of the α Relaxation for Melt-Crystallized Samples[a]

T_m (°C)	W_c	T_α (°C)	$\Delta\epsilon(T_\alpha)$	T_g (°C)
(a) Samples Cooled Continuously from the Melt at 1 °C/min				
350	0.40	163.0	0.42	150.7
375	0.38	164.0	0.50	152.6
400	0.38	163.5	0.50	152.1
(b) Samples Cooled Stepwise from the Melt in 10 °C Increments				
350	0.43	160.0	0.43	150.6
375	0.42	165.0	0.48	152.3
400	0.42	165.0	0.49	154.8

[a] T_m (°C), melt temperature; W_c, weight fraction crystallinity based on density gradient measurements; T_α (°C), isochronal peak temperature measured at 1 kHz; $\Delta\epsilon(T_\alpha) = \epsilon_r - \epsilon_u$, dielectric relaxation strength evaluated at T_α; T_g (°C), glass transition temperature measured by calorimetry (20 °C/min, DSC).

studies by Lee and Porter[10] indicate a significant influence of prior melt history on the crystallization characteristics of the material for melt temperatures in the range 370–420 °C (see also Jonas and Legras[11]). Two crystallization cooling histories were imposed from the melt: (i) continuous cooling of the sample from T_m at a rate of 1 °C/min or (ii) cooling from T_m in stepwise increments. In the latter case, samples were cooled at 1 °C/min to 330 °C, at which temperature they were annealed isothermally for 1 h. The samples were then isothermally annealed at decreasing 10 °C increments (1 h at 320, 310 °C, etc.) to 250 °C, at which point they were cooled to room temperature; this cooling progression was imposed in an effort to establish a slow cooling history within the operational constraints of the melt press.

The results of density gradient, dielectric, and DSC characterization of the melt-crystallized samples are provided in Table II; only the α (glass–rubber) relaxation was examined. The bulk levels of crystallinity achieved through melt crystallization are higher than the maximum obtainable through cold crystallization, with the highest degrees of crystallinity obtained by incremental cooling from the melt. While the range of prior melt temperatures appears to have little influence on the level of bulk crystallinity achieved in the samples, it does have a considerable impact on the observed dielectric relaxation strength across the glass transition. Specifically, $\Delta\epsilon(T_\alpha)$ increases significantly for the T_m = 375 and 400 °C samples as compared to the T_m = 350 °C specimen over both cooling histories. This increased degree of dipolar mobilization across the glass transition is most likely a reflection of the removal of prior crystalline morphology in the as-received PEEK pellets. Although the observed calorimetric melting temperature of the material is approximately 340 °C,[2] its thermodynamic melting temperature is 395 °C.[29] Thus, we would expect a full and complete erasure of prior crystallinity only in the samples prepared at 400 °C.

By a combination of cold-crystallization and melt-crystallization histories, PEEK samples with crystalline fractions ranging from 24% to 42% have been established. The measured dielectric relaxation strength across the glass transition varies directly with bulk crystallinity, as indicated by a plot of $\Delta\epsilon(T_\alpha)$ versus sample density (Figure 7). Although the available range of crystallinities is limited, the data for the crystallized samples suggest a linear extrapolation to $\Delta\epsilon = 0$ at $\rho = 1.400$ g/cm^3 (100% crystallinity). The failure of the linear extrapolation to pass through the measured amorphous specimen value for dielectric relaxation strength at $\rho_a = 1.258$ g/cm^3 indicates that the reduction in $\Delta\epsilon$ observed with crystallinity exceeds that which would result from a simple proportional relationship. This behavior is consistent with

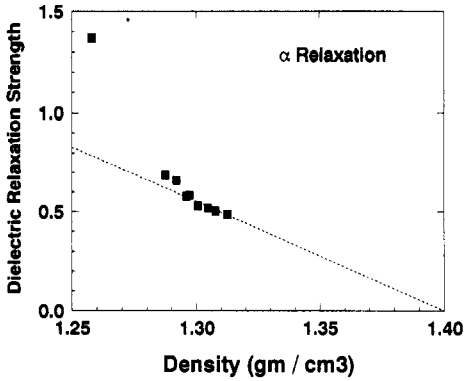

Figure 7. Dielectric relaxation strength ($\Delta\epsilon = \epsilon_r - \epsilon_u$; α relaxation) versus sample density (g/cm^3) for amorphous, cold-crystallized, and melt-crystallized PEEK.

the existence of a finite rigid amorphous fraction over the range of semicrystalline samples examined, in agreement with the calorimetric results discussed above.[2,14]

Comparison of the measured dielectric relaxation strengths of the various semicrystalline samples at their respective (α) transition temperatures relative to the relaxation strength of the amorphous sample allows for an estimation of the fraction of mobile amorphous dipoles at the glass transition in these specimens. Specifically, the weight fraction of mobile amorphous material, W_{MA}, can be determined from:[14,19]

$$W_{MA} = \frac{\Delta\epsilon(T)}{\Delta\epsilon^A(T)} \quad (2)$$

where $\Delta\epsilon(T)$ corresponds to the dielectric relaxation strength at the relaxation temperature for the (semicrystalline) material of interest, and $\Delta\epsilon^A(T)$ corresponds to the dielectric relaxation strength for an initially-amorphous specimen at the same temperature. For the calculations presented here, the relaxation temperature is designated as the maximum in the isochronal loss curve at a frequency of 1 kHz (T_α; see Table I). The determination of W_{MA} is complicated by the temperature dependence of the dielectric relaxation strength for the amorphous specimen (Figure 4a). The glass–rubber relaxation temperatures (T_α) of the semicrystalline samples fall in the range 163.5–168.5 °C; $\Delta\epsilon^A(T_\alpha)$ cannot be determined directly in this range owing to the onset of cold crystallization in the amorphous sample. Examination of Figure 4a reveals, however, that the apparent plateau in relaxation strength as a function of temperature for the amorphous material can be reasonably extrapolated into the transition range of the semicrystalline samples. Using a constant value $\Delta\epsilon^A(T_\alpha) \sim 1.15$, W_{MA} is estimated according to eq 2. The mobile amorphous fraction decreases with increasing crystallinity (in accord with Figure 7), varying from a value $W_{MA} = 0.60$ (cold-crystallized sample; T_c = 175 °C) to $W_{MA} = 0.43$ (melt-crystallized sample; slow-cooled).

Combination of the crystalline fractions determined via density measurement (W_c) and the mobile amorphous fractions estimated via dielectric relaxation (W_{MA}) allows an approximation of the amount of rigid amorphous material present in the samples at the glass transition. Specifically, the weight fraction of rigid amorphous material (W_{RAP}) can be determined by difference:

$$W_{RAP} = 1 - W_{MA} - W_C \quad (3)$$

The application of eq 3 for the estimation of the rigid amorphous fraction is limited by the uncertainty inherent in the calculation of W_{MA} owing to the necessary extrapolation of amorphous specimen relaxation strength. Also, the determination of weight fraction crystallinity (W_c) is based on the assumption that the density of the rigid amorphous fraction is the same as the density of the amorphous material (ρ_a); the validity of this approximation has been confirmed by Cebe for PPS,[20] in which the rigid amorphous phase density was found to be only slightly greater than that of the wholly-amorphous material. For the various cold-crystallized samples examined here, the estimated rigid amorphous fraction is nearly constant, $W_{RAP} = 0.185 \pm 0.025$; the relative constancy of the values reflects opposing trends in the weight fraction crystallinity and the mobile amorphous fraction as a function of increasing cold-crystallization annealing temperature. For the melt-crystallized samples, a finite rigid amorphous fraction is indicated for all specimens, with values somewhat lower than those observed for the cold-crystallization histories. For the least restrictive melt-crystallization conditions (T_m = 400 °C; slow cooling), $W_{RAP} = 0.15$.

Discussion

The dielectric characteristics of PEEK reported here are largely consistent with those observed for semicrystalline polymers of low crystallinity[27] and are in good agreement with the α relaxation results of Huo and Cebe.[14] The glass transition behavior of the material displays a strong dependence on morphology as developed over both cold-crystallization and melt-crystallization histories. Samples cold-crystallized at varying isothermal annealing temperatures display a systematic increase in crystalline fraction with T_a and a corresponding decrease in dielectric relaxation strength across the α relaxation. Relaxation temperatures based on both isochronal loss curves and calorimetric data are offset to higher temperatures in the crystallized samples and exhibit a relative maximum with crystalline fraction, T_α and T_g (DSC) decreasing at the highest cold-crystalline levels. A similar result has been observed for PET[28] and has been attributed to an increase in the thickness of the amorphous layer with increasing crystal thickness, thus reducing the relative constraint on the amorphous phase for long-range segmental motions at higher crystallinities.[32] Also, a significant broadening is observed for the α relaxation in the presence of crystallinity, with the Cole–Cole broadening parameter (β') reduced to a value of approximately 0.30 for the various cold-crystallized samples. The magnitude of the activation energies for the amorphous and cold-crystallized samples across the α relaxation reflects the cooperative nature of the molecular motions in the rubbery state, with the relaxation data following a WLF-type dependence. The cold-crystallized specimens display somewhat higher apparent activation energies as compared to the wholly-amorphous material, presumably as a reflection of the constraining influence of the crystallites on the mobile amorphous chains.

An examination of the glass transition relaxation strength as a function of crystallinity for the cold-crystallized samples reveals a decrease in $\Delta\epsilon$ which is disproportionate relative to the fraction of crystallinity present. That is, the value determined for the mobile amorphous fraction (W_{MA}) is significantly lower than would be anticipated based on the immobilization of only those dipoles incorporated into the crystalline phase. The impact of the crystallites thus appears to extend well into the noncrystalline material, which is consistent with the offset in the transition temperature observed for the semicrystalline samples. This disproportionate decrease in the dielectric relaxation intensity can be interpreted

either in terms of a decrease in the Onsager–Kirkwood correlation factor (**g**)[31] for the amorphous phase fraction of the semicrystalline samples as compared to the wholly-amorphous material or through the consideration of an immobilized rigid amorphous fraction.

The Onsager–Kirkwood correlation factor, **g**, accounts for the impact of intra- and intermolecular correlations on the response of the individual constituent dipoles and can reflect local dipolar cancellations, for example, or possible spatial restrictions to dipolar orientation. Dielectric studies by Coburn and Boyd[28] on PET demonstrated that the presence of crystallinity produced a marked decrease in the value of **g** across the glass transition as compared to that determined for the wholly-amorphous material. This result led to the conclusion that the presence of the crystalline phase not only influenced the relaxation times of the amorphous material (as reflected in the shift of the relaxation temperature) but reduced the accessibility of spatial configurations as well. The behavior observed here for the α relaxation in PEEK can be explained in a similar manner, the reduction in dielectric intensity in the semicrystalline samples reflecting both the immobilization of the crystalline phase proper and a decrease in the correlation factor for the response of the amorphous phase dipoles.

Alternatively, this behavior can be interpreted in terms of the presence of a finite, rigid amorphous fraction which remains immobilized across the glass transition; the relative fraction of rigid amorphous material can be estimated by difference based on the measured crystalline fraction (W_c) and the mobile amorphous fraction (W_{MA}) as determined by the dielectric relaxation strength. Inherent to the calculation of W_{MA} according to eq 2 is the assumption that the relaxation characteristics of the mobile amorphous phase in the semicrystalline material are satisfactorily described by the measured dielectric relaxation of the wholly-amorphous sample. This implies that the orientational correlation factor for mobile dipoles in the amorphous phase is the same for both the quenched and crystallized materials. Within the context of this model, a rigid amorphous fraction of approximately 0.185 is indicated for the cold-crystallized samples, with lower values estimated for the melt-crystallized specimens ($W_{RAP} \sim 0.15$), as reported above.

The approximation of rigid amorphous phase fraction provides a means by which to compare the calorimetric data reported previously with the measured dielectric response across the glass transition. The essentially constant value of the rigid amorphous fraction determined here for the cold-crystallized samples is intermediate between the ranges reported by Cheng et al.[2] and Huo and Cebe;[14] the dielectric data fail to reflect the decrease in the rigid amorphous phase fraction with increasing annealing temperature which is clearly demonstrated in both sets of calorimetric data, however. A finite rigid amorphous phase fraction is evident for the melt-crystallized samples, in contrast to the results of Cheng,[2] who reported the complete absence of rigid amorphous material for comparable melt-crystallization histories.

The dielectric β relaxation in PEEK displays a sensitivity to morphology which is not typically observed for sub-glass relaxations in semicrystalline polymers. Studies on the sub-glass (β) relaxation in PET,[27,28] for example, indicate that the both the location (relaxation temperature) and shape of the β relaxation are unchanged for the semicrystalline specimens as compared to the wholly-amorphous material. Further, the dielectric relaxation strength decreases in direct proportion to the crystalline fraction present, extrapolating to zero relaxation strength at 100% crystallinity. These characteristics are consistent with highly-localized, noncooperative motions in the amorphous phase which are insensitive to the presence of the crystalline fraction. In the case of PEEK, the location of the β relaxation is sensitive to the presence of crystallinity, with the maxima in dielectric loss shifted to markedly higher temperatures for the semicrystalline samples as compared to the amorphous specimen. The resulting relaxation temperatures (T_β) for the various cold-crystallized samples are largely independent of the quantity of crystallinity present, however. The lack of any clear trend in the values of T_β as a function of the degree of crystallinity may in part be a reflection of the considerable breadth of the β relaxation, which makes a precise discernment of the isochronal loss maxima difficult for the semicrystalline samples.

Examination of the dielectric relaxation strength for the β relaxation in semicrystalline PEEK reveals a reduction in relaxation strength as compared to the wholly-amorphous sample which is considerably greater than would be expected based solely on the immobilization of the crystalline phase dipoles. Specifically, the dielectric relaxation strength in the semicrystalline samples reflects a reduction in dielectric response of 60–65% as compared to the wholly-amorphous material; this reduction is observed over a crystallinity range of 24–37% (weight basis). This result, in conjunction with the observed positive shift in relaxation temperatures, indicates that the influence of the crystalline phase extends into the amorphous material, constraining to some degree the motions inherent to the β relaxation. This constraint would likely lead to a reduction in the correlation factor (**g**) relative to the dielectric response of the amorphous specimen, which is consistent with the observed reduction in relaxation strength.

The β relaxation results imply that the spatial extent of the motions inherent to the sub-glass relaxation in the semicrystalline PEEK samples is significantly greater than is encountered in polymers such as PET; this may be a reflection of the relative stiffness of the PEEK backbone. The dielectric studies of Starkweather and Avakian[21] on amorphous PEEK indicate an activation entropy close to zero for the motions inherent to the (dielectric) β relaxation, which suggests that dielectric measurements are sensitive to highly-localized, noncooperative motions along the polymer chains. Calculational studies by Chen and co-workers[33] show that the activation energy associated with isolated, crankshaft motions are consistent with the dielectric results of Starkweather. In the dielectric data presented here, the apparent activation energy determined for the amorphous sample is higher than that reported by Starkweather and Avakian but is still much lower than the value indicated for dynamic mechanical measurements, $E_a \sim 85$ kJ/mol.[21] The cold-crystallized samples examined in this work display an increase in activation energy (66 versus 58 kJ/mol for the amorphous case) which is consistent with the constraint that the crystalline phase apparently imposes on the active amorphous dipoles. Thus, in the case of the semicrystalline samples, the dielectric β relaxation appears to encompass segmental motions of longer range and greater cooperation than have been previously observed.

Conclusions

The dielectric relaxation characteristics of amorphous and semicrystalline PEEK have been investigated across a wide range of temperature and time scale; both cold-

crystallized and melt-crystallized samples were examined. Relaxation parameters based on the symmetric Cole–Cole equation have been established for the glass–rubber (α) relaxation and a sub-glass (β) relaxation. Both relaxations were sensitive to the presence of crystallinity, with the maxima in the isochronal loss curves shifting to higher temperatures in the crystallized samples. Measurement of the dielectric relaxation strength across the α relaxation indicated a reduction in relaxation strength with crystallinity which was consistent with a decrease in the orientational correlation factor for the amorphous phase dipoles; this behavior was a result of the constraint imposed by the crystalline phase on the motion of the noncrystalline dipoles and reflected what was most likely a gradient of immobilization in the vicinity of the crystal surface. The constraint of the amorphous phase dipoles by the crystalline phase was analyzed in terms of a finite rigid amorphous phase fraction for the purposes of comparing the dielectric results with available calorimetric data. The dielectric data indicated a rigid amorphous fraction $W_{RAP} = 0.185$ for the cold-crystallized samples, intermediate to values reported previously. A finite rigid amorphous fraction was also observed for the melt-crystallized samples, in contrast to previous calorimetric results. Examination of the β relaxation in PEEK also revealed an influence of crystalline morphology on dielectric response, again reflecting the constraining effect of the crystallites on the amorphous phase motions. The influence of morphology on the β relaxation in semicrystalline PEEK is in contrast to the insensitivity of sub-glass relaxations to crystallinity observed in polymers such as PET and suggests that the motions inherent to the β relaxation in PEEK encompass a larger segmental length scale than might otherwise be anticipated.

Acknowledgment. This work was supported by a graduate research assistantship (R.K.K.) through the Center for Robotics and Manufacturing Systems at the University of Kentucky.

References and Notes

(1) Medellin-Rodriguez, F. J.; Phillips, P. J. *Polym. Eng. Sci.* **1990**, *30*, 860.
(2) Cheng, S. Z. D.; Cao, M. Y.; Wunderlich, B. *Macromolecules* **1986**, *19*, 1868.
(3) Bassett, D. C.; Olley, R. H.; Al Raheil, I. A. M. *Polymer* **1988**, *29*, 1745.
(4) Lee, Y.; Porter, R. S.; Lin, J. S. *Macromolecules* **1989**, *22*, 1756.
(5) Kemmish, D. J.; Hay, J. N. *Polymer* **1985**, *26*, 905.
(6) Cebe, P.; Hong, S. *Polymer* **1986**, *27*, 1183.
(7) Day, M.; Deslandes, Y.; Roovers, J.; Suprunchuk, T. *Polymer* **1991**, *32*, 1258.
(8) Velisaris, C. N.; Seferis, J. C. *Polym. Eng. Sci.* **1986**, *26*, 1574.
(9) Cebe, P. *Polym. Eng. Sci.* **1988**, *28*, 1192.
(10) Lee, Y.; Porter, R. S. *Macromolecules* **1988**, *21*, 2770.
(11) Jonas, A.; Legras, R. *Polymer* **1991**, *32*, 2691.
(12) Jonas, A.; Legras, R.; Issi, J.-P. *Polymer* **1991**, *32*, 3364.
(13) Marand, H.; Prasad, A. *Macromolecules* **1992**, *25*, 1731.
(14) Huo, P.; Cebe P. *Macromolecules* **1992**, *25*, 902.
(15) Grebowicz, J.; Lau, S. F.; Wunderlich, B. *J. Polym. Sci., Polym. Symp.* **1984**, *71*, 19.
(16) Suzuki, H.; Grebowicz, J.; Wunderlich, B. *Makromol. Chem.* **1985**, *186*, 1109.
(17) Suzuki, H.; Wunderlich, B. *Br. Polym. J.* **1985**, *17*, 1.
(18) Cheng, S. Z. D.; Wu, Z.; Wunderlich, B. *Macromolecules* **1987**, *20*, 2802.
(19) Huo, P.; Cebe, P. *J. Polym. Sci., Polym. Phys. Ed.* **1992**, *30*, 239.
(20) Huo, P.; Cebe, P. *Colloid. Polym. Sci.* **1992**, *270*, 840.
(21) Starkweather, H. W.; Avakian, P. *Macromolecules* **1989**, *22*, 4060.
(22) D'Amore, A.; Kenny, J. M.; Nicolais, L.; Tucci, V. *Polym. Eng. Sci.* **1990**, *30*, 314.
(23) Goodwin, A. A.; Hay, J. N. *Polym. Commun.* **1989**, *30*, 288.
(24) Stober, E. J.; Seferis, J. C.; Keenan, J. D. *Polym. Eng. Sci.* **1984**, *25*, 1845.
(25) Sasuga, T.; Hagiwara, M. *Polymer* **1985**, *26*, 501.
(26) Sasuga, T.; Hagiwara, M. *Polymer* **1986**, *27*, 821.
(27) Boyd, R. H. *Polymer* **1985**, *26*, 323.
(28) Coburn, J. C.; Boyd, R. H. *Macromolecules* **1986**, *19*, 2238.
(29) Blundell, D. J.; Osborn, B. N. *Polymer* **1983**, *24*, 953.
(30) Kalika, D. S.; Yoon, D. Y. *Macromolecules* **1991**, *24*, 3404.
(31) McCrum, N. G.; Read, B. E.; Williams, G. *Anelastic and Dielectric Effects in Polymeric Solids*; John Wiley and Sons: New York, 1967.
(32) Illers, K. H.; Breuer, H. *J. Colloid Sci.* **1963**, *18*, 1.
(33) Chen, C. L.; Chang, J. L.; Su, A. C. *Macromolecules* **1992**, *25*, 1941.